

Type of the Paper (Original Research)

Spatial Footprint Distribution of Some Heavy Metals in Major Transport Routes in Ramadi City, Iraq

Rafraf Abdulaziz Abdulqader and Sufyan Mohammed Shartooh†

Department of Biology, College of Science, University of Anbar, Ramadi, Iraq

†Corresponding author: Sufyan Mohammed Shartooh; dralwaisi@uoanbar.edu.iq

ORCID: <https://orcid.org/0000-0001-5227-9072>

Key Words	Heavy metals, Road dust, Bioaccumulation, Pollution indices, Ecological risk, Arid environment, Vehicular emissions, Bioconcentration factor (BCF).
DOI	https://doi.org/10.46488/NEPT.2026.v25i04.D1936 (DOI will be active only after the final publication of the paper)
Citation for the Paper	Abdulqader, R.A. and Shartooh, S.M., 2026. Spatial footprint distribution of some heavy metals in major transport routes in Ramadi City, Iraq, <i>Nature Environment and Pollution Technology</i> , 25(4), D1936. https://doi.org/10.46488/NEPT.2026.v25i04.D1936

ABSTRACT

Rapid urbanization and industrial activity in arid regions can increase the accumulation of heavy metals (HMs) in road dust. This issue is particularly relevant in arid urban environments, where limited rainfall and frequent dust resuspension may enhance the persistence and redistribution of metal-contaminated particles. This study aimed to assess the accumulation of HMs (Zn, Cu, Cr, Pb, and Cd) in road dust and roadside vegetation of Ramadi City, Iraq. Road dust and plant samples were collected from highway, industrial, mixed-use, and residential roads, along with a control site located away from major traffic and industrial activity. The samples were digested using a tri-acid mixture, and metal concentrations were determined by flame atomic absorption spectroscopy. Road-dust contamination was evaluated using the Geo-accumulation Index (Igeo), Pollution Load Index (PLI), Degree of Contamination (CD), Potential Ecological Risk Index (PERI), and Integrated Pollution Index (IPI). The efficiency of plants to accumulate metals from road dust was estimated using the bioconcentration factor (BCF). Statistical analysis showed significant spatial variation among road categories, suggesting anthropogenic enrichment ($p \leq 0.01$). Industrial and mixed-use sites generally showed the highest contamination and ecological risk levels, while residential sites showed lower but still detectable metal accumulation. The levels of heavy metals in plant tissue were reported in the following abundance order: Zn > Cr > Cu > Pb > Cd; both Cd and Cr exceeded the reported permissible limits. The BCF values were below 1 for all studied metals, indicating that the sampled vegetation behaved

mainly as a metal excluder rather than a hyperaccumulator. The high aridity of the climate in Ramadi may contribute to the persistence and redistribution of metal-contaminated dust through aeolian transport, particularly from industrial and traffic-intensive areas toward adjacent urban zones. The findings highlight the need for regular monitoring, dust-control measures, and source-reduction strategies to limit further accumulation and potential ecological exposure in arid urban environments.

1. INTRODUCTION

Environmental pollution remains a major global concern because of its effects on ecosystem quality and human health. Among the different classes of pollutants, heavy metals are of particular concern because they are persistent, non-biodegradable, and capable of accumulating in environmental media and biological tissues (Landrigan et al. 2018; Shartooh et al. 2018).

Heavy metals are environmental contaminants that can affect soil quality, vegetation, animals, and humans, depending on their concentration, chemical form, exposure route, and duration of exposure. The primary sources of heavy metal pollution are industrial emissions and human activities. Heavy metals may occur naturally in soils through parent-material weathering, but elevated concentrations are often associated with anthropogenic inputs (Alloway 2012). Important anthropogenic sources include industrial emissions, fuel combustion, vehicle exhaust, brake wear, tyre wear, waste disposal and resuspension of contaminated dust (El-Sergany et al. 2011). Fine particle-size fractions of dust and soil are good indicators of the bioavailability of metals and may be more relevant for exposure assessment than bulk soil samples due to their higher potential for dermal adherence and either inhalation or ingestion (Madrid et al., 2008; Arunachalam et al., 2026).

Furthermore, heavy metals can act as environmental stressors that affect plant growth and physiological functioning. When metal concentrations exceed their natural levels in the soil, they impose pervasive and toxic effects on the entire plant system (Bharti & Sharma 2022). Plants can absorb metals through the root system and may also retain metal-bearing particles deposited on leaf surfaces. Their presence becomes toxic when their concentration increases within the plant tissue, changing the plant's capacity to uptake and accumulate non-essential elements that may cause direct and/or indirect effects that harm plant health (Musa et al. 2024). The presence of these metals in the food chain constitutes a serious threat to health (Ali & Khan 2019). Soil pollution with HMs resulting from petrochemical processes can affect ecosystems and may create exposure pathways through contaminated vegetation (Gupta et al. 2022).

Road dust pollution with HMs poses an important environmental concern in urban areas because fossil fuel combustion, industrial activity, moving vehicles, tire wear, brake wear, and road-surface abrasion generate metal-containing particles. Road type is an important factor in determining the intensity of emissions sources and human activities, and in estimating heavy-metal concentrations. Higher concentrations are often reported on industrial and highway roads compared to residential and agricultural roads. This is due to direct emissions from factories, storage operations, heavy truck traffic, tire wear, and fuel use. In residential areas, pollution sources are mainly associated with local traffic emissions and home heating. Mixed-use roads may show elevated contamination because traffic emissions, commercial activity, and small-scale workshops can occur in the same area (He et al. 2021). Additionally, exposure may occur through skin contact, respiratory inhalation, and ingestion via the food chain. Long-term exposure to metal-contaminated dust has been associated with adverse health outcomes, although the level of risk depends on metal concentration, particle size, exposure frequency, and population vulnerability (Lu et al. 2025).

Ramadi City is located in an arid region of Iraq where limited rainfall, high temperatures, and frequent dust events may favor the accumulation and redistribution of contaminated road dust. The city also includes major transport routes, residential zones, mixed-use areas, and industrial activities, making it suitable for examining how road function influences heavy-metal distribution. However, information on heavy-metal contamination in road dust and associated roadside vegetation in Ramadi remains limited. Therefore, this study assessed the spatial distribution of Zn, Cu, Cr, Pb, and Cd in road dust and roadside vegetation along major transport routes in Ramadi City. The study also applied multiple pollution indices and the bioconcentration factor to evaluate contamination status, ecological risk, and metal transfer from road dust to vegetation.

2. MATERIALS AND METHODS

2.1. Study area description

Ramadi City, one of the major cities of Anbar Governorate, is located in west-central Iraq. Anbar covers approximately one-third of Iraq's total land area, and Ramadi serves as an important urban and transport hub along the Euphrates River. Its significance is further increased by its location on major international transit routes connecting Iraq with neighboring countries. The region is characterized by a desert climate, with high temperatures and minimal precipitation throughout the year. These climatic conditions, particularly low rainfall and frequent dust events, play a crucial role in

the accumulation and distribution of heavy metals in road dust (Al-Bayati & Al-Ani 2025). The route locations were recorded using a Garmin 72 GPS.

2.2. Sample collection

In Ramadi City, road dust samples were collected systematically from four road categories: highway, industrial, mixed-use, and residential roads. Highways were defined as high-speed transport routes with relatively high volumes of heavy-duty vehicles. Industrial roads were located close to industrial activities and workshops. Mixed-use roads included both commercial and moderate volumes of traffic, while residential roads were found within areas with lower overall traffic volumes. The plant species *Conocarpus erectus* was selected to assess heavy-metal accumulation in road-side vegetation and to calculate bioconcentration factor (BCF) values. Its widespread presence in all sample collection areas during the current study, coupled with its evergreen nature and tolerance to the arid conditions characteristic of the study area, made it a suitable choice. Previously, it has been used to estimate heavy metals in soils in several countries (Rastmanesh et al. 2024). Furthermore, it is considered an important bioindicator of heavy metal pollution due to its ability to accumulate metals within harvestable plant parts and its high bioconcentration ratio (Almehdi et al. 2019).

Each of the four road categories was sampled at five sites, designated L1, L2, L3, L4, and L5. At each site, three subsamples were collected and analyzed to form one composite road-dust sample. Thus, 20 composite road-dust samples were collected, along with 20 plant samples from vegetation adjacent to the corresponding road-dust sampling sites. A control site (CS) was selected approximately 18 km away from industrial plumes and traffic emissions to provide baseline values for comparison (Table 1; Fig. 1). This allowed comparison between road-influenced sites and background conditions with limited direct influence from traffic or industrial activity. Road dust was collected using a plastic broom and dustpan to prevent contamination from metallic sampling tools. After collection, all sampled materials were placed in pre-labelled airtight bags and transported to the laboratory, where they were then dried, sieved using 106 μm sieve, and chemically analyzed (Ali et al. 2025).

Table 1: Information of the sample collection sites.

	Road category																				
Road type	Highway					Industrial					Mixed					Residential					
Location	L1	L2	L3	L4	L5	L1	L2	L3	L4	L5	L1	L2	L3	L4	L5	L1	L2	L3	L4	L5	CS

GPS	
X	Y
43.205695	33.445410
43.275278	33.456697
43.339003	33.421914
43.302407	33.459403
43.338220	33.486448
43.303272	33.430989
43.316158	33.430187
43.273999	33.408665
43.258501	33.419081
43.214356	33.432431
43.274312	33.412072
43.301877	33.421860
43.244838	33.420433
43.336124	33.429674
43.294679	33.422424
43.333915	33.430782
43.296651	33.432110
43.302854	33.419093
43.318106	33.408433
43.198298	33.409003
43.204796	33.405785

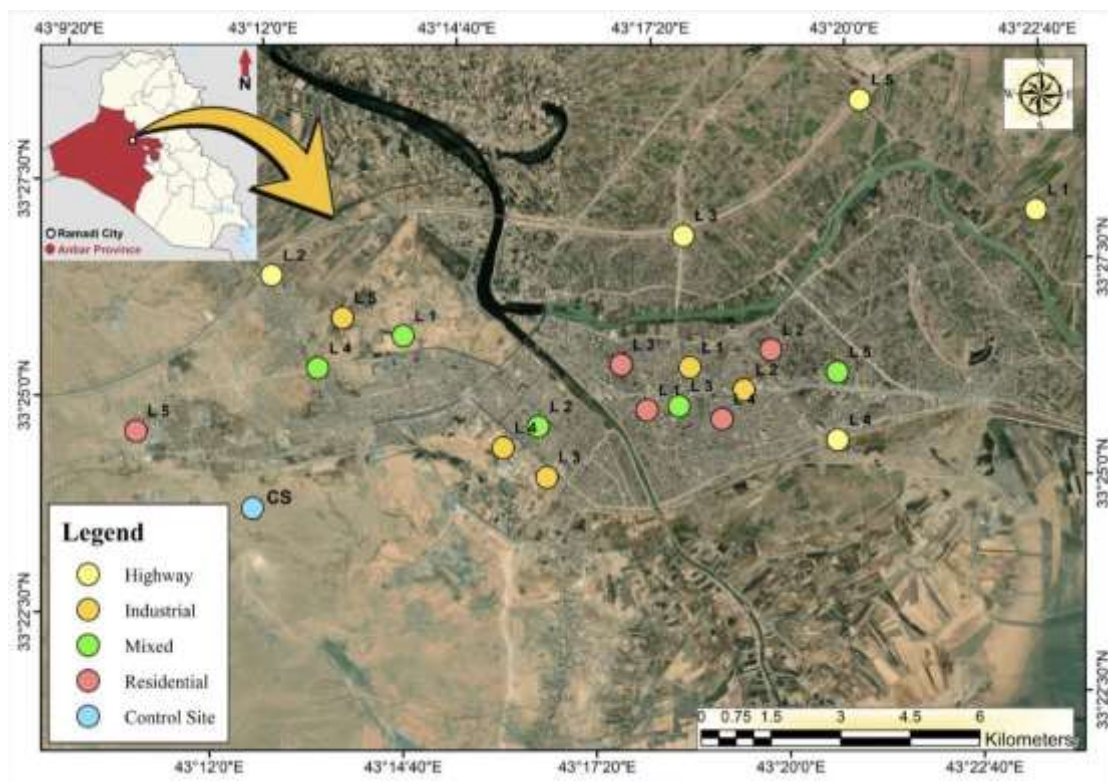


Fig. 1: Location map of the selected sampling routes.

Samples were dried at 105°C for 24 hours and sieved through a 106 µm sieve; the fraction smaller than 106 µm was selected for analysis. Vegetation samples were also collected from areas adjacent to the road-dust sampling sites to determine the concentrations of the studied heavy metals in above-ground plant tissues. One gram of each oven-dried and ground plant and road-dust sample was digested at 80°C with 15 mL of a tri-acid mixture containing HNO₃, H₂SO₄, and HClO₄ in a 4.5:1:1 ratio. The mixture was stirred until homogeneous.

Subsequently, the mixture was placed in a microwave system where the power, temperature, and time were set according to the conditions specified in Table 2. Upon completion of the digestion period, the mixture was left to cool,

filtered using Whatman filter paper grade 595, and adjusted to a volume of 50 mL by adding distilled water (Chandel & Bharose 2020).

Table 2: Microwave conditions.

Temperature	Energy	Time	Volume	Mixture of acids
150°C	1050 W	20 min	15 mL	HNO ₃ :H ₂ SO ₄ :HClO ₄ , 4.5:1:1

2.4. Standard solutions and flame atomic absorption spectroscopy analysis

Standard solutions of 1000 mg/L of Zn, Cu, Cr, Pb, and Cd were prepared by dissolving the required mass of each corresponding metal salt in 1 L of deionized distilled water (DDW). The solutions were stored in glass containers at 4°C for further analysis. The optimal operating conditions for the flame atomic absorption spectroscopy (FAAS) system (AA-7000, Shimadzu, Japan) were established, with the specific limit of detection (LOD), limit of quantification (LOQ), wavelength, and flame type for each analyzed element detailed in Table 3 (Zhang 2024). For the quantification process, a series of working standard solutions was prepared by diluting a 1000 mg/L stock solution to cover the expected concentration range of the analytes, as specified in the calibration data shown in Table 3. Since the digested sample solutions exhibited an acidic pH ranging from 4.0 to 6.5, which can influence the flow rate within the nebulizer, the standard solutions were similarly acidified with 4–5 drops of concentrated nitric acid HNO₃ to ensure matrix matching and consistent aspiration. Elemental concentrations were then measured using FAAS.

Table 3: Flame atomic absorption spectrometer calibration data.

Element	Wavelength (nm)	Flame type Air/Acetylene	LOD (mg/L)	LOQ (mg/L)
Pb	217	Ordinary fuel	0.003	0.021
Cd	228.8	Ordinary fuel	0.002	0.014
Cu	324.8	Poor fuel	0.004	0.021
Cr	357.9	Rich fuel	0.005	0.035
Zn	213.9	Poor fuel	0.003	0.021

2.5. Pollution assessment methods

A geochemical assessment was used to evaluate heavy metal (Zn, Cu, Cr, Pb, and Cd) contamination levels in Ramadi road dust. Five environmental indices were used to assess contamination intensity and possible anthropogenic enrichment: 1) Geo-accumulation index (I-geo), 2) Pollution load index (PLI), 3) Degree of contamination (CD), 4) Potential ecological risk index (PERI), and 5) Integrated pollution index (IPI).

For plants, the bioconcentration factor was used to assess the accumulation of metals (i.e., Zn, Cu, Cr, Pb, Cd) in their tissues. BCF was calculated as the ratio of the metal concentration in plant tissue to the concentration of the same metal in the corresponding road-dust sample.

2.5.1. Geo-accumulation Index (*I-geo*)

The Geo-accumulation Index (*I-geo*) is an established geochemical index for assessing metal contamination in all types of environmental media, including road dust (Gałuszka & Migaszewski 2025). The *I-geo* measures the concentration of one element in a sample relative to its natural or pre-industrial background level. Thus, it provides an indication of metal enrichment relative to background conditions. The formula for calculating *I-geo* is as equation: (1) (Islam et al. 2020).

$$I_{geo} = \log_2 \left(\frac{C_m}{1.5 B_m} \right) \quad \dots (1)$$

where C_m represents the concentration of metals in the road-dust sample, while B_m denotes the background value of the same metals. To account for potential fluctuations in the background data, a factor of 1.5 was applied, enhancing the reliability of the comparison against baseline values. The values can then be categorized into different pollution classes (Alghanimi et al. 2024), as in Table 4.

Table 4: Geo-accumulation index levels

<i>I_{geo}</i> Class	<i>I_{geo}</i> Value	Contamination category
0	$I_{geo} \leq 0$	Uncontaminated
1	$I_{geo} 0-1$	Uncontaminated to moderately contaminated
2	$I_{geo} 1-2$	Moderately contaminated
3	$I_{geo} 2-3$	Moderately to strongly contaminated
4	$I_{geo} 3-4$	Strongly contaminated
5	$I_{geo} 4-5$	Strongly to very strongly contaminated
6	$I_{geo} > 5$	Very strongly contaminated

2.5.2. Pollution Load Index (*PLI*)

The Pollution Load Index is a geochemical tool used to determine the collective level of heavy metal contamination in soil, sediment and dust. Unlike individual contamination factors, the PLI provides a comprehensive summary of the total pollution burden at a site (Skvarekova et al. 2021). The Contamination Factor (CF) and PLI were calculated using the following equations (2), (3) (Tomlinson et al. 1980):

$$CF = \frac{C_m}{B_m} \quad \dots (2)$$

$$PLI = (CF_1 \times CF_2 \times CF_3 \times CF_4 \times CF_5 \times \dots \times CF_n)^{1/n} \quad \dots (3)$$

where C_m represents the metal concentration in road dust, B_m is the background value of the metal, n represents the number of elements. PLI value of less than 1 indicates no pollution, whereas a value greater than 1 indicates pollution (Pancholi et al. 2022).

2.5.3. Contamination Degree (CD)

The Contamination Degree (CD) is a cumulative index that quantifies the total intensity of pollution by summing the contamination factors of all individual metals identified at a sampling location. It provides an estimate of the overall contamination burden relative to background values and was calculated using equation (4) (Hosseinzadeh et al. 2024). Additionally, the degree of contamination was classified into four categories as given in Table 5.

$$CD = \sum_{i=1}^{i=n} CF \quad \dots (4)$$

Table 5: The Contamination Degree classes.

Contamination Degree	Contamination Degree Categories
$CD < 8$	Low level of contamination
$8 \leq CD < 16$	Moderate degree of contamination
$16 \leq CD < 32$	Significant degree of contamination
$CD \geq 32$	Very high degree of contamination

2.5.4. Potential Ecological Risk Index (PERI)

The Potential Ecological Risk Index is a commonly used to evaluate the degree of heavy metal pollution in sediments, soils, and urban dust. Unlike simple enrichment factors, the PERI integrates the concentration of pollutants with their biological toxicity, providing an estimate of potential ecological risk. The PERI is calculated using the following equations (5)-(7) (Xie et al. 2023):

$$C_f^i = \frac{C_d^i}{C_r^i} \quad \dots (5)$$

$$ER = E_r^i = T_r^i \times C_f^i \quad \dots (6)$$

$$PERI = \sum_{i=1}^n E_r^i \quad \dots (7)$$

where $C_{i;d}$ represents the measured concentration of metal i in road dust, $C_{i;r}$ is the background value of metal i , $C_{i;f}$ is the contamination factor, $T_{i;r}$ is the toxic-response factor, and $E_{i;r}$ is the ecological risk factor for each metal. Toxic response factors for Zn, Cu, Cr, Pb, and Cd are 1, 5, 2, 5, and 30, respectively (Hakanson 1980). The PERI categories were classified as follows: $RI < 150$ indicates low risk, $150 < RI < 300$ indicates moderate risk, $300 < RI < 600$ reflects a considerable ecological risk, and an $RI > 600$ signifies a very high ecological risk (El-Sharkawy et al. 2025).

2.5.5. Integrated Pollution Index (IPI)

The Integrated Pollution Index (IPI) is a comprehensive numerical tool used to assess the overall quality of a specific medium (usually soil, water, or air) by calculating the combined effects of multiple pollutants, most commonly heavy metals. In this study, it was used to assess the cumulative heavy-metal pollution level in road dust. The IPI was calculated using equations (8) and (9) (Mansouri et al. 2024):

$$PI = \frac{C_n}{B_n} \quad \dots (8)$$

$$IPI = \frac{1}{n} \sum_{i=1}^n PI_i \quad \dots (9)$$

where C_n refers to the measured concentration in the sample, B_n is the background concentration of the heavy metal in the Earth's crust, and n is the number of metals studied. The IPI is calculated as the average of all pollution indices (PI) for the metals considered and values are classified as low contamination ($IPI \leq 1.0$), moderately contaminated ($1.0 < IPI \leq 2.0$), or highly contaminated ($IPI > 2.0$) (Cobbina et al. 2025).

2.5.6. Bioconcentration factor (BCF)

The bioconcentration factor is used to measure the ability of plants to absorb and accumulate heavy metals from soil and dust, providing a direct indication of metal bioavailability to vegetation (Aladesanmi et al. 2019). To quantify the enrichment of HMs in plant tissue, the following equation was used (10) (Chen et al. 2024):

$$BCF = \frac{C_{leave}}{C_{soil}} \quad \dots (10)$$

where C_{leave} represents the metal concentration in the leaf/plant tissue, C_{soil} represents the metal concentration in the road-dust sample. The BCF refers to the ratio of the heavy metal concentration in a plant to that in road dust. BCF values

greater than 1 indicate greater metal accumulation in plant tissue relative to the surrounding substrate, whereas BCF values below 1 indicate limited accumulation or exclusion behavior.

2.5.7. Statistical analysis

One-way analysis of variance (ANOVA) was used to analyze differences in metal concentrations among road categories and sampling locations. SPSS software (version 25) was used for statistical analyses, with $p \leq 0.01$ considered statistically significant.

The choice of background values is a key factor in interpreting geochemical data. Previous studies have used the average shale values (Mohiuddin et al. 2011; Salam et al. 2021; Tnoumi et al. 2022; Al-Dahar et al. 2023; Rasul et al. 2026), or the upper continental crust (UCC) data (Xuefeng et al. 2016; Tang et al. 2019; Dytlow & Gorka 2021; Hamid et al. 2022) as reference baselines. The estimated concentrations of the elements were compared with the geochemical background values of the UCC given by (Rudnick & Gao 2003). The permissible limits in soil and plant are presented in (Table 6).

Figures were generated and formatted using Python 3.13.5. Data importing and preprocessing were performed using pandas and NumPy, curve smoothing was carried out using SciPy, and graphical rendering and export were completed using Matplotlib.

Table 6: The background values and permissible limits of under study elements

Element	Background values (ppm)	Soil permissible limits* (ppm)	Plant permissible limits* (ppm)
Zn	65.4	50	0.6
Cu	22.5	36	10
Cr	67.3	100	1.3
Pb	20	85	2
Cd	0.3	0.8	0.02

**According to WHO (1996)*

3. RESULTS AND DISCUSSIONS

3.1. Heavy metal concentrations in road dust

Table 7 presents the mean values \pm standard deviation of Zn, Cu, Cr, Pb and Cd in road-dust samples collected from highway, industrial, mixed-use, and residential roads in Ramadi City, along with a control sample collected away from major transport routes.

Table 7: Mean heavy metals concentration (ppm) \pm standard deviation (SD) in road-dust samples collected from different road categories in Al-Ramadi city.

Road Type	Locations	Heavy metal concentration in ppm (Mean \pm SD)				
		Zn	Cu	Cr	Pb	Cd
Highway Road	L 1	59.1 \pm 6.7	20.5 \pm 2.9	15.0 \pm 1.5	20.5 \pm 3.7	2.69 \pm 0.78
	L 2	50.1 \pm 6.3	21.4 \pm 3.0	18.0 \pm 2.0	41.4 \pm 3.8	2.5 \pm 0.71
	L 3	42.9 \pm 4.5	31.9 \pm 3.1	16.2 \pm 1.6	27.6 \pm 3.2	1.94 \pm 0.56
	L 4	45.0 \pm 4.2	24.3 \pm 2.2	17.0 \pm 1.0	30.5 \pm 2.9	2.8 \pm 0.78
	L 5	55.0 \pm 4.8	30.0 \pm 2.4	14.5 \pm 1.9	25.9 \pm 3.1	1.99 \pm 0.67
Industrial roads	L 1	70.3 \pm 7.9	141.8 \pm 18.6	23.0 \pm 3.0	232.9 \pm 51.7	3.15 \pm 0.81
	L 2	66.7 \pm 5.5	210.5 \pm 53.5	26.5 \pm 3.7	115.6 \pm 42.4	3.15 \pm 1.07
	L 3	56.2 \pm 4.8	33.5 \pm 2.9	18.8 \pm 2.4	38.3 \pm 4.2	2.69 \pm 0.89
	L 4	54.3 \pm 5.0	32.3 \pm 4.1	19.6 \pm 2.8	48.0 \pm 4.0	2.85 \pm 0.57
	L 5	60.2 \pm 4.96	40.5 \pm 4.7	25.3 \pm 2.9	85.9 \pm 6.9	3.0 \pm 1.3
Mixed Road	L 1	55.9 \pm 4.3	14.8 \pm 1.2	17.7 \pm 2.1	30.2 \pm 2.9	3.1 \pm 0.91
	L 2	58.4 \pm 5.2	21.0 \pm 1.9	21.9 \pm 1.7	53.2 \pm 4.8	2.85 \pm 0.77
	L 3	66.7 \pm 5.9	33.7 \pm 3.5	21.0 \pm 1.9	49.0 \pm 4.6	3.46 \pm 1.02
	L 4	37.0 \pm 2.8	11.5 \pm 1.3	15.0 \pm 2.0	21.4 \pm 2.8	2.15 \pm 0.93
	L 5	62.3 \pm 5.7	25.5 \pm 2.9	19.2 \pm 2.4	45.1 \pm 3.9	3.5 \pm 1.06
Residential roads	L 1	53.2 \pm 4.8	13.8 \pm 1.6	16.2 \pm 1.8	50.7 \pm 3.7	2.38 \pm 0.96
	L 2	38.5 \pm 2.9	8.5 \pm 0.95	14.7 \pm 1.1	20.7 \pm 2.5	2.1 \pm 0.91
	L 3	32.5 \pm 3.7	10.2 \pm 1.2	18.3 \pm 1.9	30.5 \pm 3.5	2.5 \pm 0.7
	L 4	35.5 \pm 3.7	8.2 \pm 1.02	8.0 \pm 1.2	20.0 \pm 3.2	2.1 \pm 0.8
	L 5	26.0 \pm 1.6	6.3 \pm 0.27	8.7 \pm 0.9	16.0 \pm 1.2	1.93 \pm 0.17
Control	C	34.5 \pm 3.5	13.7 \pm 2.9	19.8 \pm 2.4	17.8 \pm 2.2	1.6 \pm 0.8

The analytical findings showed elevated concentrations of Zinc, Copper, Chromium, Lead, and Cadmium across most road categories compared with the control site. The highest concentrations of Cu and Pb were observed at industrial sites, particularly L1 and L2, while Cd showed consistently elevated values across the highway, industrial, mixed-use, and residential road categories. Statistical significance at $p \leq 0.01$ indicates clear spatial variation among sampling locations and suggests a strong influence of likely anthropogenic sources such as industrial activity, traffic emissions, brake and tyre wear, and road-dust resuspension (Kilavi et al. 2023). Overall, industrial roads showed the strongest enrichment for Cu and Pb, whereas residential roads generally recorded the lowest concentrations for most metals.

The road-adjacent samples show a distinct gradient of pollution when compared with control samples. For example, Pb at industrial site L1 was much higher than the control value, indicating localized enrichment near industrial activity. Such enrichment is consistent with previous observations that urban soils and road dust in rapidly growing cities may accumulate metals above background levels, especially near traffic and industrial sources (Adimalla 2020). Low levels of contamination near residential roads may reflect lower traffic density and greater separation from direct industrial sources (Du et al. 2026). However, some metals were still detectable at residential sites, suggesting possible redistribution of metal-bearing dust from traffic-intensive or industrial areas. Fine particulate (PM_{2.5}) and/or coarse

particulate matter (PM10) with high heavy metal concentrations can travel in excess of several kilometers from an industrial site to an adjacent residential or commercial area (Zurek-Ost et al. 2025).

The significant difference between road categories and the control site indicates that road function and surrounding land use influence heavy-metal accumulation in road dust. The results also indicate localized contamination hotspots, especially at industrial sites with high Cu and Pb concentrations. The concentration of cadmium exceeded the reported permissible limit across all road categories, while Pb exceeded the permissible limit at some industrial sites. These findings suggest that Cd and Pb require particular attention in future monitoring and risk assessment. The results indicate that road dust in Ramadi City is affected by multi-metal contamination, with the highest burden generally observed near industrial and high-traffic routes. The statistically significant differences among sites ($p \leq 0.01$) support the interpretation that metal distribution is spatially structured rather than random. However, further source apportionment and exposure assessment studies would be needed to determine specific emission sources and potential health risks.

3.2. Heavy-metal concentrations in roadside vegetation

Mean concentration values \pm standard deviation of Zn, Cu, Cr, Pb, and Cd in plant samples collected from highway, industrial, mixed-use, and residential roads in Ramadi City are presented in Table 8.

Table 8: Mean heavy metals (ppm) \pm Standard deviation in plant samples collected from 5 locations adjacent to different roads within Al-Ramadi city.

Road Type	Locations	Heavy Metal Concentration in ppm (Mean \pm SD)				
		Zn	Cu	Cr	Pb	Cd
Highway Road	L 1	18.5 \pm 2.8	3.5 \pm 1.7	2.86 \pm 0.78	2.0 \pm 0.38	0.38 \pm 0.06
	L 2	18.4 \pm 2.2	5.5 \pm 1.9	4.5 \pm 1.1	2.0 \pm 0.62	0.54 \pm 0.04
	L 3	16.9 \pm 2.5	5.1 \pm 1.08	5.72 \pm 2.14	3.0 \pm 0.9	0.33 \pm 0.07
	L 4	17.0 \pm 2.1	4.9 \pm 1.36	3.8 \pm 0.78	2.5 \pm 0.8	0.44 \pm 0.04
	L 5	15.8 \pm 1.8	4.5 \pm 1.22	2.9 \pm 0.93	1.99 \pm 0.9	0.39 \pm 0.01
Indus. Road	L 1	14.0 \pm 1.2	2.9 \pm 1.01	3.76 \pm 1.37	2.5 \pm 1.1	0.38 \pm 0.06
	L 2	22.9 \pm 2.3	2.5 \pm 0.95	2.15 \pm 0.95	2.5 \pm 1.7	0.39 \pm 0.03
	L 3	20.0 \pm 1.9	2.7 \pm 0.99	2.73 \pm 0.89	1.95 \pm 0.5	0.32 \pm 0.04
	L 4	14.0 \pm 1.6	3.0 \pm 0.98	3.14 \pm 1.06	2.0 \pm 0.95	0.33 \pm 0.03
	L 5	21.5 \pm 2.9	3.2 \pm 1.4	2.69 \pm 1.09	2.2 \pm 0.86	0.32 \pm 0.04
Mixed Road	L 1	24.8 \pm 3.4	2.8 \pm 1.2	2.86 \pm 0.96	2.2 \pm 0.76	0.69 \pm 0.05
	L 2	23.8 \pm 2.6	3.0 \pm 1.3	3.86 \pm 1.22	1.91 \pm 0.93	0.54 \pm 0.06
	L 3	12.0 \pm 0.6	2.5 \pm 0.97	2.85 \pm 1.09	1.88 \pm 1.0	0.31 \pm 0.05
	L 4	12.0 \pm 0.9	3.6 \pm 1.44	2.71 \pm 0.91	1.82 \pm 0.94	0.23 \pm 0.03
	L 5	18.9 \pm 1.9	2.9 \pm 1.6	3.95 \pm 1.03	1.99 \pm 0.79	0.6 \pm 0.08
Reside. Road	L 1	17.2 \pm 2.0	2.5 \pm 1.02	3.43 \pm 1.11	1.78 \pm 0.34	0.15 \pm 0.03
	L 2	10.5 \pm 0.9	2.42 \pm 0.94	2.86 \pm 0.74	1.79 \pm 0.71	0.15 \pm 0.05

L 3	19.0±2.2	2.5±1.0	3.15±1.07	1.8±0.62	0.3±0.03
L 4	14.8±1.8	2.5±0.93	2.14±0.92	1.52±0.66	0.22±0.06
L 5	9.9±1.7	1.82±0.84	2.72±0.94	1.78±0.48	0.35±0.09

The results identified mixed road L1 and highway L3 as locations with relatively high metal accumulation in plant tissue. In mixed roads, Zn and Cd reached the highest concentrations of 24.8 ppm and 0.69 ppm, respectively, at L1, where mixed-use roads in Ramadi City are associated with stop-and-go traffic and informal mechanical workshops. Plants in such zones may accumulate metals through both root uptake from contaminated substrate and foliar deposition of resuspended particulates (Al-Dahar et al. 2023; Giri et al. 2026). Cd, in particular, is relatively mobile in some soil-plant systems and may be taken up by plant tissues depending on soil chemistry and metal availability. Roadside flora in high-traffic commercial zones may show elevated Cd accumulation where traffic activity, lubricants, battery waste, or small mechanical workshops contribute to local contamination (Bhatla & Kathpalia 2023). Cr and Pb in highways (L3) recorded the peak for Cr (5.72 ppm) and Pb (3.0 ppm). These elevated concentrations may be related to traffic-derived particles from brake wear, tyre wear, exhaust emissions, and resuspended dust; however, the present study does not directly identify the specific source contribution for each metal (Bhat et al. 2025).

Mixed-use and highway sites showed relatively high accumulation for selected metals, probably reflecting the density and diversity of nearby pollution sources (Rahman et al. 2024). The interaction between location and metal type was found to be highly significant ($p \leq 0.01$) for Cr, Pb, and Cd. Plant Cd concentrations ranged from 0.15 to 0.69 ppm, with the maximum value recorded at mixed-use site L1; therefore, the value of approximately 3.5 ppm appears to refer to Cd in road dust rather than plant tissue. This pattern may be associated with differences in local traffic intensity, commercial activity, and the availability of Cd in road dust. In mixed roads, the combination of high-density traffic with frequent braking and local commercial activities may create a persistent source of Cd. Cadmium can occur as an impurity in low-grade automotive lubricants and certain tire brands. Furthermore, mixed-use zones in Ramadi City may include small mechanical workshops where oil residues and dust deposition contribute to localized contamination (Horne & Fleming-Singer 2005; Panda et al. 2025). In semi-arid regions, the high evaporation rate may increase the concentration of Cd ions in the soil's pore water, thereby influencing the bioconcentration factor in roadside flora (Giri et al. 2026). Residential roads generally showed lower accumulation for most metals, which may reflect lower traffic intensity and reduced exposure to heavy-duty vehicle emissions. The reduced concentration of re-suspended dust may limit the foliar uptake of metals. Urban green belts in residential zones can act as filters, although they may still accumulate metals at rates higher than natural baselines (Basheer et al. 2026).

The difference between the control site and road-adjacent locations indicates that traffic and urban activity are likely contributors to metal accumulation in roadside vegetation. Since the control site approximately reflects the natural background of the region, higher concentrations in road-adjacent plants may be associated with atmospheric deposition, dust resuspension, and transport-related emissions (Bhat et al. 2025). Comparison with a control site strengthens the interpretation that road-adjacent vegetation is exposed to additional metal inputs, although source-specific confirmation would require further analysis (Edo et al. 2024; Naeem et al. 2024). Generally, the plants along major roads in Ramadi City accumulated Cr, Pb, and Cd at levels exceeding the reported permissible limits for some metals. The ANOVA results indicate significant spatial differences in plant metal concentrations; however, proximity to traffic should be interpreted as a likely contributing factor rather than the sole determinant (Hussain et al. 2024). The relatively higher concentrations of Zn and Cu may also reflect their role as essential micronutrients, although excessive levels can still affect plant function (Rahman et al. 2024).

3.3. Road-dust contamination indices

3.3.1. Geo-accumulation Index (*I_{geo}*)

Fig. 2 shows the values of *I_{geo}* of all examined heavy metals in road-dust samples collected from five locations across highway, industrial, mixed-use, and residential roads. The highest *I_{geo}* values were generally recorded for Cd, followed by Pb and Cu at selected industrial and mixed-use sites, whereas Cr consistently showed the lowest *I_{geo}* values across the examined locations.

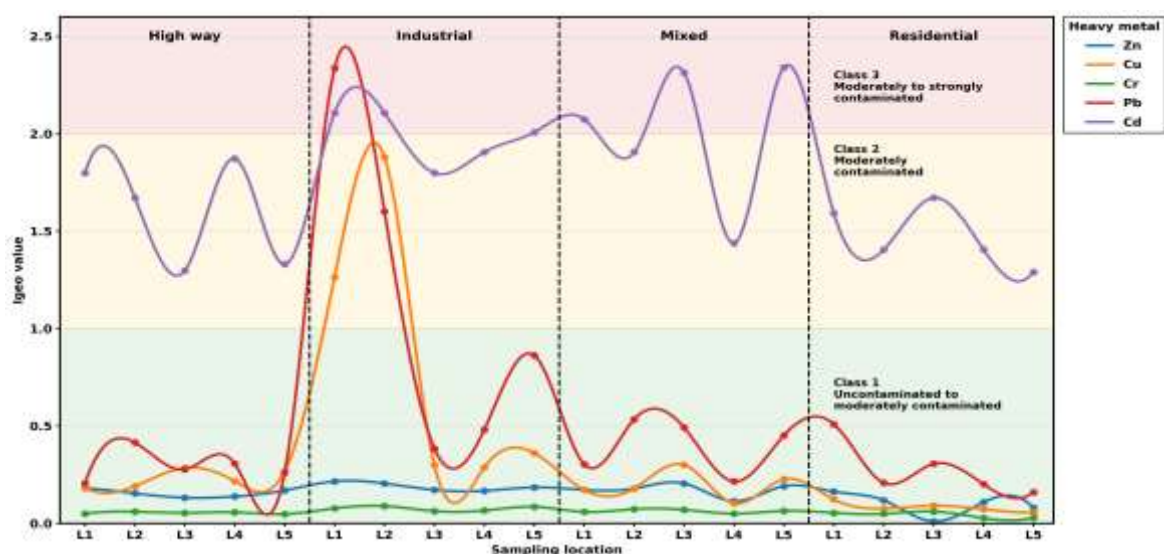


Fig. 2: Igeo values of the examined heavy metals in road-dust samples collected from highway, industrial, mixed-use, and residential roads

The Igeo results indicate that industrial sites were most affected by Pb and Cu enrichment. Industrial L1 showed the highest Pb Igeo value, while industrial L2 showed the highest Cu Igeo value. This may be associated with the persistence of environmental contaminants linked to previous fuel-related emissions, traffic activity, and ongoing discharges from mechanical or metal-processing activities near industrial roads (Generalova et al., 2025). However, source-specific attribution should be treated cautiously because no direct source-apportionment analysis was conducted.

For highway sites, Igeo values for Zn, Cu, Cr, and Pb were mostly below 1, indicating uncontaminated to moderately contaminated conditions. In contrast, Cd showed higher Igeo values, indicating moderate contamination at several highway locations. Roadside dust samples have Igeo values of less than 1.0, except when they are affected by industrial activity. Therefore, highway sites are affected by vehicle emissions, but their enrichment levels for most metals remained lower than those observed at the most contaminated industrial sites. Furthermore, residential road-dust samples have the lowest Igeo values for all elements. Most of the Igeo values for chromium and zinc are close to zero, indicating low enrichment relative to background values. However, lead at residential L1 showed moderate enrichment compared with other residential locations. The residential sites may also receive metal-bearing particulates through atmospheric transport and local traffic activity. Cadmium and lead consistently have higher Igeo values than chromium, and chromium has the lowest Igeo values for all sites.

3.4. Other road-dust contamination indices

Values of pollution load index (PLI), contamination degree (CD), potential ecological risk index (PERI), and integrated pollution index (IPI) in road-dust samples collected from five locations along highway, industrial, mixed-use, and residential roads showed clear variation among sampling sites and road categories. Among the calculated indices, CD and IPI showed the largest numerical ranges, while PLI values were comparatively lower because the index is expressed as a geometric mean of contamination factors.

3.4.1. Pollution load index (PLI)

The results indicate that industrial and mixed road sites were the most heavily impacted by anthropogenic activities, with industrial sites recording the highest PLI values, specifically L1 and L2 (Fig. 3).

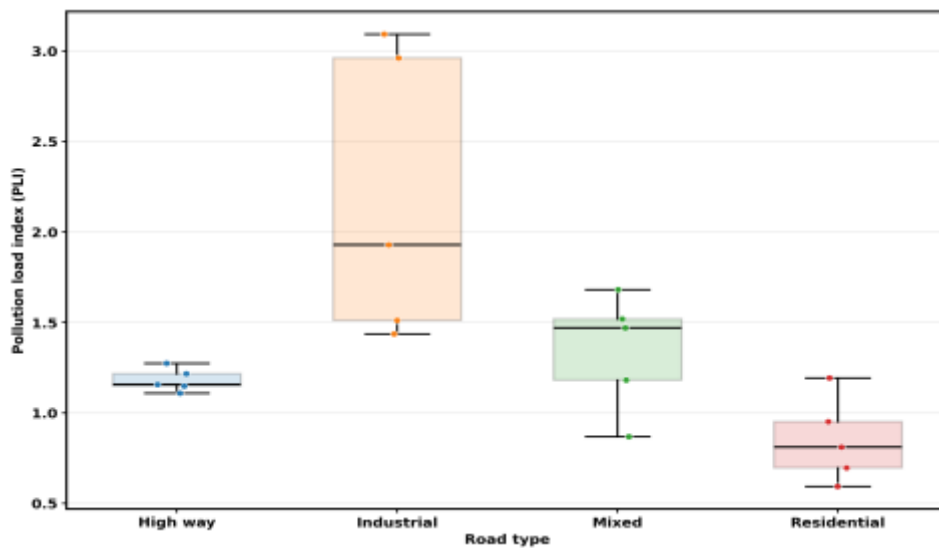


Fig. 3: Pollution load index (PLI) distribution by road type

The highest PLI value was recorded at industrial L1 (3.09), followed by industrial L2 (2.96), indicating a high overall pollution load at these sites (Ali et al. 2025). PLI values above 3 are commonly interpreted as evidence of substantial anthropogenic contamination, particularly in areas influenced by industrial activity, mechanical workshops, or metal-processing sources. Most mixed-use road sites also showed PLI values greater than 1, indicating pollution relative to background conditions (Barbera et al. 2025). The obtained data suggest that mixed-use zones may experience cumulative inputs from traffic emissions, commercial activity, and small-scale workshops, which together increase the overall pollution load (Attiya & Jones 2020).

The highway areas had a consistent level of pollution across the five sampling locations, with PLI values slightly above 1 at all sites. These values indicate low to moderate pollution, probably associated with continuous deposition from traffic-related sources such as exhaust emissions, brake wear, tyre wear, and road-surface abrasion (Al-Sabbagh & Shreaz 2025). Highway road-dust samples with PLI values ranging from 1.0 to 1.5 indicate early-stage contamination and support the need for periodic monitoring (Atavullayeva 2024).

In contrast, residential sites generally showed lower PLI values, with most locations below 1, indicating limited pollution according to the PLI classification. However, the value at residential L1 exceeded 1, suggesting localized enrichment or possible influence from nearby traffic or dust transport (Miller et al. 2025). Such localized elevation may also occur when fine particulate matter is transported from nearby industrial or traffic-intensive areas under favorable wind conditions (Afandi et al. 2025).

3.4.2. Contamination degree (CD)

The highest CD values were recorded at industrial road sites, particularly L1 and L2 (Fig. 4). The CD values at locations L1 and L2 were 29.86 and 27.05, respectively, placing them within the significant contamination category according to the classification used in this study (Cao et al. 2025). These elevated CD values are consistent with cumulative inputs from mechanical activities, industrial emissions, and metal-processing residues (Somadas & Sarvade 2025). Although high CD values indicate strong cumulative contamination, further leaching tests and groundwater monitoring would be required before concluding that deeper soil layers or groundwater are at risk (Ogwu et al. 2025).

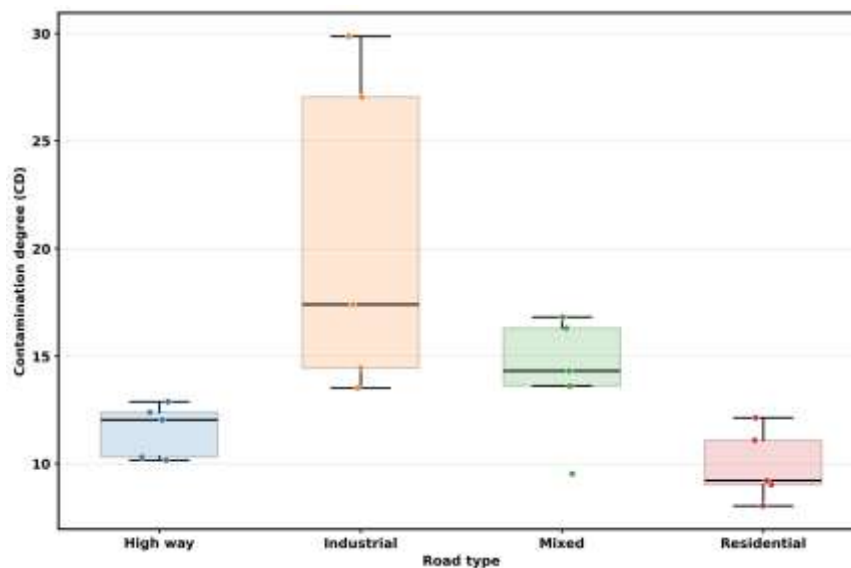


Fig. 4: Contamination degree (CD) distribution by road type

Highway and mixed-use sites showed CD values ranging from 9.53 to 16.81. The highway sites showed a relatively consistent moderate contamination range of approximately 10.1-12.8, whereas the mixed-use sites showed greater variation, especially L3, where a 16.81 CD was recorded. The bulk of contaminants for both the highway and mixed sites may originate from diffuse anthropogenic sources, including emissions from vehicles, brake pad wear, and wear from tires (Candeias et al. 2020). However, the additional increase in the mixed-use sites suggests an interaction between traffic volume and nearby commercial activities (e.g., repair shops). Areas with combined commercial and transport activity may accumulate higher metal loads because of stop-and-go traffic, vehicle maintenance activities, and small-scale metal-related sources (Jacob et al. 2024).

The residential showed the lowest CD values, mostly within the moderate contamination category (Skuzza et al. 2022). Although lower than industrial and mixed-use sites, the residential values indicate that road dust in residential areas is not entirely free from metal accumulation. This may reflect local traffic emissions, resuspended dust, and possible atmospheric transport of metal-bearing particles from more polluted areas.

3.4.3. Potential ecological risk index (PERI)

Industrial sites showed some of the highest PERI values, with several locations exceeding 300, indicating considerable ecological risk according to the classification used in this study (Barbera et al. 2025) (Fig. 5). The elevated PERI values at industrial sites are likely related to the strong contribution of metals with high toxic-response factors, particularly Cd, and to elevated Pb concentrations at selected locations (Barbera et al. 2025). Mixed-use sites L3 and L5 also recorded high PERI values, indicating considerable ecological risk (Cao et al. 2025). This pattern may reflect the combined influence of traffic emissions, commercial activity, and small-scale workshops in mixed-use areas.

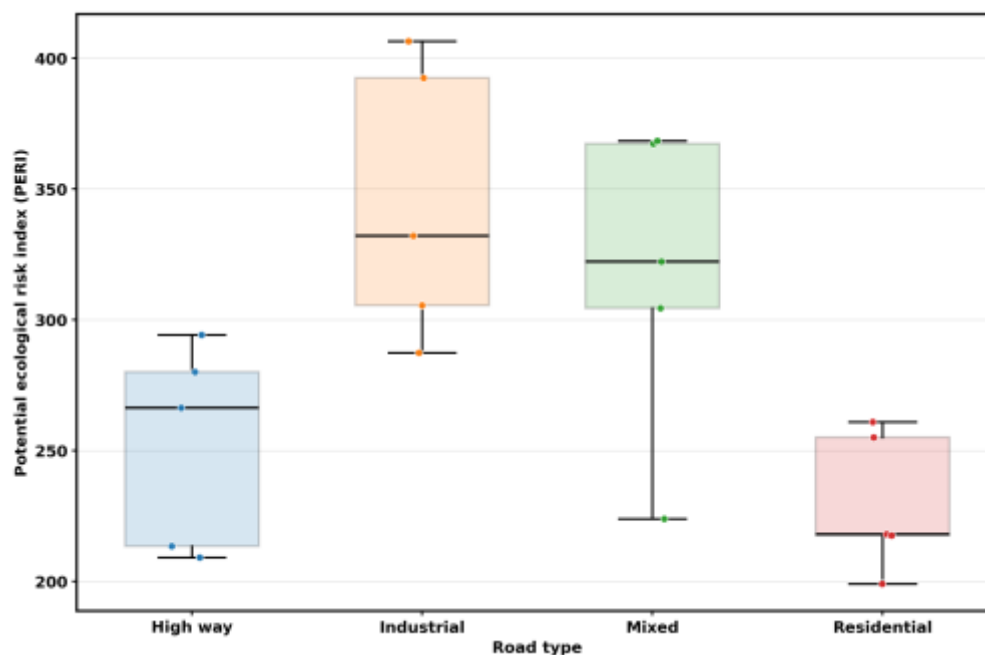


Fig. 5: Potential ecological risk index (PERI) distribution by road type

The highway and residential locations generally presented lower PERI values, though they still fell within the moderate to considerable risk categories, where the values of highway sites varied between 209.12 and 294.21. Although none of the highway sites exceeded 300, the proximity of L4 (294.21) to the considerable-risk threshold indicates a significant accumulation of traffic-related pollutants (Attiya & Jones 2020). Regarding residential sites, which showed

the lowest risk profile, all values remained above the low-risk threshold, suggesting that residential road dust may still receive metal inputs from local traffic and atmospheric deposition (Al-Sabbagh & Shreaz 2025).

3.4.4. Integrated pollution index (IPI)

The highest IPI value in the industrial category was observed at L1 with a value of 21.4639, while industrial L2 recorded 18.64919 (Fig. 6). These values indicate very high cumulative contamination at the two industrial sites. The elevated IPI values at L1 and L2 may reflect cumulative inputs from industrial emissions, mechanical wastes, and metal-processing activities (Miller et al. 2025) from industrial sources. IPI values greater than 10 indicate strong anthropogenic loading, although the specific contribution of individual sources requires further source-apportionment analysis. The results suggest that most of the locations had higher IPI values than the other road categories. (Szwalec et al. 2020).

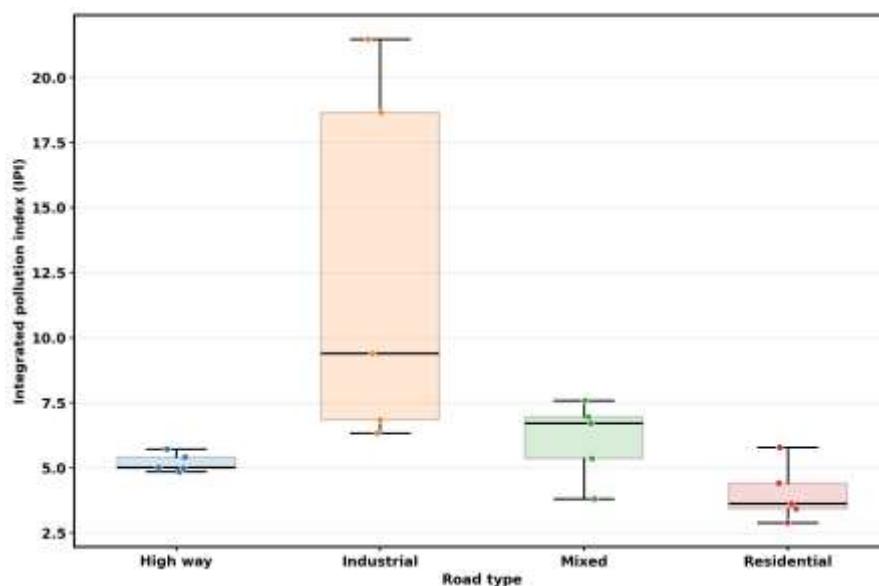


Fig. 6: Integrated pollution index (IPI) distribution by road type

Mixed-use sites L3 and L5 also showed elevated IPI values, suggesting increased cumulative contamination in areas where traffic and commercial activities overlap (Jacob et al. 2024). However, the highway system showed relatively consistent IPI values of approximately 5.0 across locations (Atavullayeva 2024), with lower variability than industrial and mixed-use sites. Urban corridors often have moderate to high IPI values because of diffuse pollution from tyre wear, brake wear, road abrasion, and fuel combustion (Candeias et al. 2020).

Residential areas showed the lowest total IPI, and while the residential IPI values at each sample point were lower than those of industrial and most mixed-use sites, all values remained above 1.0, indicating that residential road dust was not free from contamination (Szwalec et al. 2020). The highest residential sample point value at L1 (5.78) may

reflect localized traffic influence or proximity to more polluted transport corridors (Barbera et al. 2025). Overall, the IPI results confirm that industrial roads were the most contaminated, followed by mixed-use and highway roads, while residential roads showed the lowest but still measurable cumulative contamination (Attiya & Jones 2020).

3.5. Plant bioconcentration factor (BCF)

Fig. 7 presents the calculated bioconcentration factor (BCF) values for plant samples collected from five locations along highway, industrial, mixed-use, and residential roads. Overall, Zn showed the highest BCF values among the studied metals, whereas Pb generally showed the lowest BCF values across the examined locations.

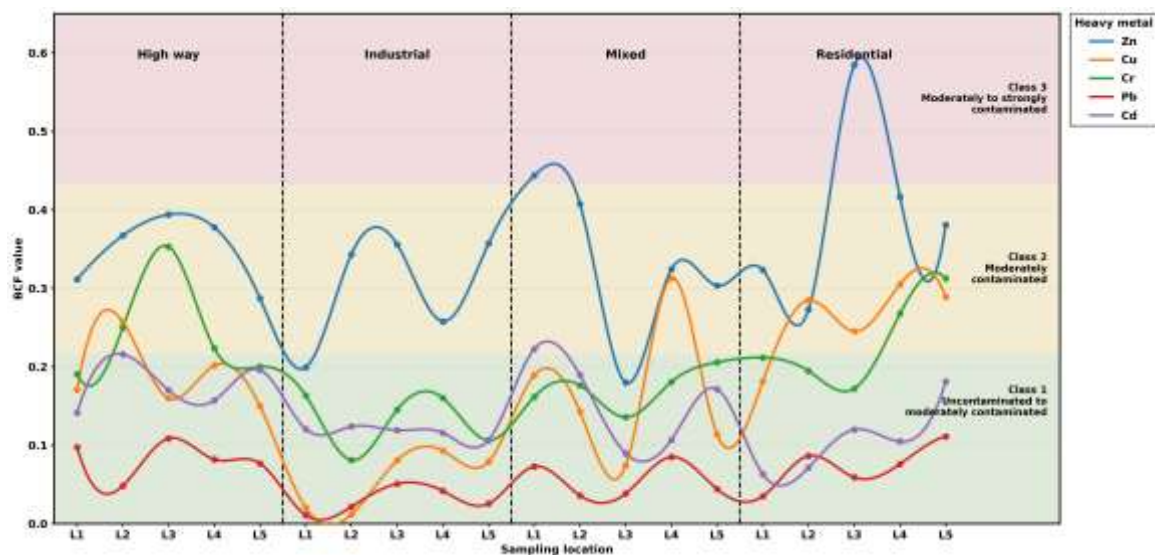


Fig. 7: Bio-concentration factor (BCF) distribution by road type and sampling location

The industrial sites showed high road-dust contamination but relatively low BCF values for several metals. At L1, the BCF for Pb was the lowest recorded value (0.010734), while the highest industrial-site value was recorded for Zn at L3 (0.355872). Plants in highly polluted industrial zones may show limited metal transfer from substrate to tissue because of exclusion mechanisms, restricted root uptake, or low metal bioavailability in the substrate (Skuzza et al. 2022; Ali et al. 2025).

Mixed-use and highway roads showed moderate BCF values for selected metals, reflecting their exposure to traffic-related and mixed anthropogenic inputs (Attiya & Jones 2020). The highway category showed relatively high BCF values for Zn and Cr at L3, and the lowest Pb BCF value at L2. The mixed-use roads showed a peak for Cu at L4 and Zn at L1, suggesting site-specific differences in metal availability and plant uptake. In traffic-affected areas, some metals

may occur in more bioavailable forms, whereas metals in industrial dust may be more strongly bound to particles or mineral phases, reducing plant uptake (Jacob et al. 2024).

However, the residential sites are the least polluted in terms of dust concentration but show surprisingly high efficiency in metal translocation. Zn recorded the highest BCF values among all examined metals, which often exhibits higher BCF values because it is an essential micronutrient for plant enzymatic functions, facilitating its active transport compared to non-essential elements like Pb, which showed the lowest BCF values across all sites. Pb has low bioavailability and tends to be sequestered in the soil-root interface, which explains the minimal BCF values observed in the under study plant samples (Ayobami 2022; Goya-Heredia et al. 2023).

Interestingly, the residential road locations showed a similar pattern of metal uptake to that observed at traffic-affected sites, with relatively higher Zn BCF values at selected locations such as residential L3. This suggests that while road-dust concentrations are higher in industrial zones, plant uptake efficiency (BCF) does not necessarily increase linearly with substrate pollution, often due to substrate pH, organic matter content, metal speciation, or particle binding (Goya-Heredia et al. 2023; Barbera et al. 2025). Because all BCF values were below 1, the sampled plants can be interpreted as metal excluders rather than hyperaccumulators.

4. CONCLUSIONS

This study provides an assessment of heavy metal contamination in road dust, and its subsequent bioaccumulation in native vegetation along four functional road categories (highway, industrial, mixed-use, and residential) in Ramadi City, Iraq. The integration of multiple pollution indices (I-geo, PLI, CD, PERI, IPI) and bioconcentration factor (BCF) analysis provided a useful framework for evaluating contamination intensity, ecological risk, and plant uptake behavior in an arid urban setting.

The results showed that road-adjacent dust samples generally contained higher heavy metal concentrations than the control site, suggesting the influence of anthropogenic sources. The highest contamination burden was generally observed at industrial sites, particularly for Cu and Pb, while Cd showed consistent enrichment across several road categories. Significant spatial differences ($p \leq 0.01$) indicate that road type and surrounding land use influenced heavy-metal distribution. The PERI classified most road categories within moderate to considerable ecological-risk levels, with industrial and mixed-use sites showing the highest values. The Igeo ranked Cd as the most enriched element across most

sites, followed by Pb, indicating notable enrichment relative to background values. The PLI, CD, and IPI results further confirmed that industrial roads had the greatest cumulative contamination, followed by mixed-use and highway roads, whereas residential roads showed lower but still measurable contamination.

Although the BCF remained below 1 for all metals suggesting that plants act as excluders rather than hyperaccumulators, the absolute concentrations of Cd and Cr in plant biomass exceeded the reported permissible limits. This indicates that roadside vegetation can serve as an indicator of metal exposure in contaminated road environments, although further studies are required to assess grazing, food-chain transfer, and human-health risks. The arid climate of Ramadi City may enhance the persistence and redistribution of contaminated dust because low rainfall and frequent dust events can favor aeolian transport and resuspension of metal-bearing particles. The detection of metals in residential road dust suggests that lower-traffic areas may still receive inputs from local traffic, dust movement, or nearby polluted zones.

Overall, the results of the present study highlight the need for regular road-dust monitoring, control of industrial and traffic-related emissions, improved dust-management practices, and further source-apportionment and exposure-assessment studies in Ramadi City and similar arid urban environments.

Author Contributions: Conceptualization, S.M.; methodology, S.M.; software, S.M.; validation, R.A. and S.M.; formal analysis, R.A. and S.M.; investigation, R.A.; resources, R.A.; data curation, R.A. and S.M.; writing—original draft preparation, R.A. and S.M.; writing—review and editing, R.A. and S.M.; visualization, S.M.; supervision, S.M.; project administration, S.M.; funding acquisition, S.M. Authors have read and agreed to the published version of the manuscript.

Funding: This research received no external funding.

Informed Consent Statement: Not applicable

Acknowledgments: The authors thank the staff of the Department of Biology, College of Science, University of Anbar, for their support during this work.

Conflicts of Interest: The authors declare no conflicts of interest

REFERENCES

Acheampong, S., 2023. Heavy metals' poisoning in farm animals. In: *Heavy Metals: Recent Advances*. IntechOpen. [DOI]

- Adimalla, N., 2020. Heavy metals pollution assessment and its associated human health risk evaluation of urban soils from Indian cities: A review. *Environmental Geochemistry and Health*, 42(1), pp.173-190. [\[DOI\]](#)
- Afandi, G.E., Bolden-Tiller, O., Mortley, D., Asare-Baah, L., Miller, R., Ibrahim, S. and Rangari, V., 2025. Air quality assessment and source speciation of PM_{2.5} in Florida's Everglades Agricultural Area. *Earth Systems and Environment*, pp.1-23. [\[DOI\]](#)
- Aladesanmi, O.T., Oroboade, J.G., Osisiogu, C.P. and Osewole, A.O., 2019. Bioaccumulation factor of selected heavy metals in *Zea mays*. *Journal of Health and Pollution*, 9(24), 191207. [\[DOI\]](#)
- Al-Bayati, A.H.I. and Al-Ani, M.K., 2025. Climate change and its impact on the ecosystem on the Ramadi Island Plateau for the period from 1980 to 2022. In: *International Conference Water and Food Security in the Face of Climate Change: Challenges and Opportunities for Resilience*. Springer Nature Switzerland, Cham, pp.51-66. [\[DOI\]](#)
- Al-Dahar, R.K., Rabee, A.M. and Mohammed, R.J., 2023. Calculation of soil pollution indices with elements in residential areas of Baghdad City. *Revista Bionatura*, 8(1), 43. [\[DOI\]](#)
- Alghanimi, S.M.K., Chamani, A., Almusawi, A.N. and Tavabe, K.R., 2024. Potentially toxic elements risk assessment and source identification of an at-risk international wetland in SW Iran. *Wetlands*, 44(5), 63. [\[DOI\]](#)
- Ali, H. and Khan, E., 2019. Trophic transfer, bioaccumulation and biomagnification of non-essential hazardous heavy metals and metalloids in food chains/webs: Concepts and implications for wildlife and human health. *Human and Ecological Risk Assessment: An International Journal*, 25(6), pp.1353-1376. [\[DOI\]](#)
- Ali, M., Alshamsi, D., Ahmad, T., Ahmed, A. and Abdelfadil, K.M., 2025. Assessment of potentially toxic metals (PTMs) pollution, ecological risks and source apportionment in urban soils from university campuses: Insights from multivariate and positive matrix factorisation analyses. *Minerals*, 15(5), 482. [\[DOI\]](#)
- Alloway, B.J., 2012. Sources of heavy metals and metalloids in soils. In: *Heavy Metals in Soils: Trace Metals and Metalloids in Soils and Their Bioavailability*. Springer, Dordrecht, pp.11-50. [\[DOI\]](#)
- Almejdi, A., El-Keblawy, A., Shehadi, I., El-Naggar, M., Saadoun, I., Mosa, K.A. and Abhilash, P.C., 2019. Old leaves accumulate more heavy metals than other parts of the desert shrub *Calotropis procera* at a traffic-polluted site as assessed by two analytical techniques. *International Journal of Phytoremediation*, 21(12), pp.1254-1262. [\[DOI\]](#)
- Al-Sabbagh, T.A. and Shreaz, S., 2025. Impact of lead pollution from vehicular traffic on highway-side grazing areas: Challenges and mitigation policies. *International Journal of Environmental Research and Public Health*, 22(2), 311. [\[DOI\]](#)
- Arunachalam, K.P., Hussain, S.A., Algburi, S., Sabihuddin, S., Mohammed, S.J., Majidi, H.S. and Al-Baghdadi, A.H., 2026. Eco-smart geomaterials and nano-engineered soils: Innovations in geotechnical engineering for pollution mitigation and environmental sustainability. *Nature Environment and Pollution Technology*, 25(2), D1823. [\[DOI\]](#)
- Atavullayeva, M., 2024. Environmental pollution monitoring: Essential strategies for mitigating ecological degradation. *E3S Web of Conferences*, 587, 02014. [\[DOI\]](#)
- Attiya, A.A. and Jones, B.G., 2020. Assessment of mineralogical and chemical properties of airborne dust in Iraq. *SN Applied Sciences*, 2(9), 1614. [\[DOI\]](#)
- Ayobami, A.O., 2022. An assessment of trace metal pollution indicators in soils around oil well clusters. *Petroleum Research*, 7(2), pp.275-285. [\[DOI\]](#)

- Barbera, M., Gariglio, S., Malegori, C., Oliveri, P., Saiano, F., Scalenghe, R. and Piazzese, D., 2025. Multivariate strategy for understanding soil features from rare-earth element profiles: A focus on data normalization. *ACS Measurement Science Au*, 5(2), pp.189-198. [\[DOI\]](#)
- Basheer, M.Z., Huang, X., Cai, X., Cui, Y. and Muhammad, M., 2026. Integrating chemical and microbial strategies for heavy metal remediation in contaminated soils: Opportunities, challenges and key factors. *Environmental Science and Pollution Research*, pp.1-19. [\[DOI\]](#)
- Bharti, R. and Sharma, R., 2022. Effect of heavy metals: An overview. *Materials Today: Proceedings*, 51, pp.880-885. [\[DOI\]](#)
- Bhat, B.A., Rather, M.A., Bilal, T., Nazir, R., Qadir, R.U. and Mir, R.A., 2025. Plant hyperaccumulators: A state-of-the-art review on mechanism of heavy metal transport and sequestration. *Frontiers in Plant Science*, 16, 1631378. [\[DOI\]](#)
- Bhatla, S.C. and Kathpalia, R., 2023. Essential and functional mineral elements. In: *Plant Physiology, Development and Metabolism*. Springer Nature, Singapore, pp.25-49. [\[DOI\]](#)
- Candeias, C., Vicente, E., Tomé, M., Rocha, F., Ávila, P. and Célia, A., 2020. Geochemical, mineralogical and morphological characterisation of road dust and associated health risks. *International Journal of Environmental Research and Public Health*, 17(5), 1563. [\[DOI\]](#)
- Cao, M., Tang, Q., Gai, N., Ma, S., Liu, J. and Wang, F., 2025. Contamination characteristics, source apportionment and risk assessment of heavy metals and metalloids in the soil-crop-human system within the typical high geological background region of the Yangtze River Delta. *Journal of Environmental Management*, 391, 126443. [\[DOI\]](#)
- Chandel, S.S. and Bharose, R., 2020. Evaluation of heavy metal contamination in green leafy vegetables grown in Allahabad. *International Journal of Environment, Agriculture and Biotechnology*, 5(5), pp.1220-1225. [\[DOI\]](#)
- Chen, Y., Ding, Z., Yu, T., Cao, L., Duan, Y., Zu, Y. and Li, Z., 2024. Accumulation characteristics of heavy metals in three wild rice species and adaptation of root morphology and anatomical structure to native soil heavy metals in Yunnan. *Ecological Indicators*, 167, 112601. [\[DOI\]](#)
- Cobbina, S.J., Edu, A.R., Bosso, E.E., Bampoe, E. and Gautam, S., 2025. Impact of industrial activities on soil quality in urban settings: A study of heavy metal concentrations in Lamashegu, Ghana. *Discover Soil*, 2(1), 68. [\[DOI\]](#)
- Du, X., Jiang, R., Sun, W., Tian, D. and Zheng, Z., 2026. Heavy metal risk assessment of 53-day accumulated road-deposited sediments from different roads in Beijing using Monte Carlo simulation. *Environmental Monitoring and Assessment*, 198(3), 222. [\[DOI\]](#)
- Dytlow, S. and Górka-Kostrubiec, B., 2021. Concentration of heavy metals in street dust: An implication of using different geochemical background data in estimating the level of heavy metal pollution. *Environmental Geochemistry and Health*, 43(1), pp.521-535. [\[DOI\]](#)
- Edo, G.I., Samuel, P.O., Oloni, G.O., Ezekiel, G.O., Ikpekor, V.O., Obasohan, P. and Agbo, J.J., 2024. Environmental persistence, bioaccumulation and ecotoxicology of heavy metals. *Chemistry and Ecology*, 40(3), pp.322-349. [\[DOI\]](#)
- El-Sergany, M.M. and El-Sharkawy, M.F., 2011. Heavy metal contamination of airborne dust in the environment of two main cities in the Eastern Province of Saudi Arabia. *Journal of King Abdulaziz University: Meteorology, Environment and Arid Land Agriculture Sciences*, 22(1), pp.135-148. [\[DOI\]](#)

- El-Sharkawy, G., Alotaibi, M.O., Zuhair, R., Mahmoud, E., El Baroudy, A., Omara, A.E.D. and El-Sharkawy, M., 2025. Ecological assessment of polluted soils: Linking ecological risks, soil quality and biota diversity in contaminated soils. *Sustainability*, 17(4), 1524. [\[DOI\]](#)
- Gałuszka, A. and Migaszewski, Z.M., 2025. Environmental assessment of metals in road dust: What do geochemical indices really tell us about pollution? *Environmental Geochemistry and Health*, 47(4), 128. [\[DOI\]](#)
- Generalova, A., Davidova, S. and Satchanska, G., 2025. The mechanisms of lead toxicity in living organisms. *Journal of Xenobiotics*, 15(5), 146. [\[DOI\]](#)
- Giri, S., Roy, A., Kumar, A., Ghosh, S., Bhunia, A. and Patra, S., 2026. Cadmium toxicity-related metabolic bone disease: A clinical conundrum of five cases. *Osteoporosis International*, 37(2), pp.525-531. [\[DOI\]](#)
- Goya-Heredia, A.V., Zafra-Mejía, C.A. and Rondón-Quintana, H.A., 2023. Spatial analysis of heavy metal pollution in road-deposited sediments based on the traffic intensity of a megacity. *Atmosphere*, 14(6), 1033. [\[DOI\]](#)
- Gupta, N., Yadav, K.K., Kumar, V., Prasad, S., Cabral-Pinto, M.M., Jeon, B.H. and Alsukaibia, A.K.D., 2022. Investigation of heavy metal accumulation in vegetables and health risk to humans from their consumption. *Frontiers in Environmental Science*, 10, 791052. [\[DOI\]](#)
- Hakanson, L., 1980. An ecological risk index for aquatic pollution control: A sedimentological approach. *Water Research*, 14(8), pp.975-1001. [\[DOI\]](#)
- Hamid, E., Payandeh, K., Karimi Nezhad, M.T. and Saadati, N., 2022. Potential ecological risk assessment of heavy metals/trace elements in coastal soils of southwest Iran. *Frontiers in Public Health*, 10, 889130. [\[DOI\]](#)
- He, Y., Zhang, Y., Peng, C., Wan, X., Guo, Z. and Xiao, X., 2021. Distribution characteristics and risk assessment of heavy metals in soil and street dust with different land uses: A case in Changsha, China. *International Journal of Environmental Research and Public Health*, 18(20), 10733. [\[DOI\]](#)
- Horne, A.J. and Fleming-Singer, M., 2005. Phytoremediation using constructed treatment wetlands: An overview. In: *Bioremediation of Aquatic and Terrestrial Ecosystems*. Science Publishers, Plymouth, UK, pp.329-377. [\[DOI\]](#)
- Hosseinzadeh, M., Toranjzar, H., Ahmadi, A., Abdi, N. and Varvani, J., 2024. Assessment of potentially toxic elements pollution in soils and plant leaves along the high-traffic highway zones in Tehran, Iran. *Anthropogenic Pollution*, 8(2), pp.1-16. [\[DOI\]](#)
- Hussain, B., Abbas, A., Saleem, A.R., Riaz, L., Rahman, S.U., Liu, S. and Farooq, M., 2024. Uptake, agglomeration and detoxification of trace metals and metalloids in plants. *Journal of Soil Science and Plant Nutrition*, 24(3), pp.4965-4983. [\[DOI\]](#)
- Imran, S., Sumi, M.J., Harine, I.J., Paul, N.C., Mahamud, M.A., Rabbi, R.H.M. and Rhaman, M.S., 2025. Biochar amendments in soil: A sustainable approach for mitigating heavy metal stress in plants. *Phyton-International Journal of Experimental Botany*, 94(4), pp.1073-1109. [\[DOI\]](#)
- Islam, M.S., Ahmed, M.K., Al-Mamun, M.H. and Eaton, D.W., 2020. Human and ecological risks of metals in soils under different land-use types in an urban environment of Bangladesh. *Pedosphere*, 30(2), pp.202-213. [\[DOI\]](#)
- Jacob, D.E., Nelson, I.U., Izah, S.C., Ukpong, E., Akpan, U.U. and Ogwu, M.C., 2024. Bioindicators in recreational planning and development: Balancing nature and human activities. In: *Biomonitoring of Pollutants in the Global South*. Springer Nature, Singapore, pp.835-878. [\[DOI\]](#)

- Kilavi, P.K., Kaniu, M.I., Patel, J.P. and Usman, I.T., 2023. Assessment of heavy metal pollution in soil and associated risks in the environs adjacent to a heavy mineral sand mine on the South Coast of Kenya. *Water, Air, & Soil Pollution*, 234(12), 748. [\[DOI\]](#)
- Landrigan, P.J., Fuller, R., Hu, H., Caravanos, J., Cropper, M.L., Hanrahan, D. and Suk, W.A., 2018. Pollution and global health: An agenda for prevention. *Environmental Health Perspectives*, 126(8), 084501. [\[DOI\]](#)
- Lu, H., Shen, Y., Maurya, P., Chen, J., Li, T. and Paz-Ferreiro, J., 2025. Spatial heterogeneity of heavy metals contamination in urban road dust and associated human health risks. *Land*, 14(4), 754. [\[DOI\]](#)
- Madrid, F., Biasioli, M. and Ajmone-Marsan, F., 2008. Availability and bioaccessibility of metals in fine particles of some urban soils. *Archives of Environmental Contamination and Toxicology*, 55(1), pp.21-32. [\[DOI\]](#)
- Mansouri, M.S., Payandeh, K., Koushafar, A., Goosheh, M. and Mohammadi Rouzbahani, M., 2024. Level of heavy metals and environmental pollution index in Ahvaz, Southwest Iran. *Scientific Reports*, 14(1), 14754. [\[DOI\]](#)
- Miller, T., Durlík, I., Kostecka, E., Kozłowska, P., Łobodzińska, A., Sokołowska, S. and Nowy, A., 2025. Integrating artificial intelligence agents with the internet of things for enhanced environmental monitoring: Applications in water quality and climate data. *Electronics*, 14(4), 696. [\[DOI\]](#)
- Mohiuddin, K.M., Ogawa, Y., Zakir, H.M., Otomo, K. and Shikazono, N., 2011. Heavy metals contamination in water and sediments of an urban river in a developing country. *International Journal of Environmental Science and Technology*, 8(4), pp.723-736. [\[DOI\]](#)
- Musa, I.O., Ijah, U.J.J., Abioye, O.P., Abdulsalam, M., Pal, S.K., Abamhekelu, I.A. and Akande, S.A., 2024. Phytoremediation of heavy metal-contaminated soil. In: *Eco-restoration of Polluted Environment*. CRC Press, pp.35-52. [\[DOI\]](#)
- Naeem, M.A., Shabbir, A., Imran, M., Ahmad, S., Shahid, M., Murtaza, B. and Khan, W.U.D., 2024. Silicon-nanoparticles loaded biochar for soil arsenic immobilization and alleviation of phytotoxicity in barley: Implications for human health risk. *Environmental Science and Pollution Research*, 31(16), pp.23591-23609. [\[DOI\]](#)
- Ogwu, M.C., Izah, S.C., Sawyer, W.E. and Amabie, T., 2025. Environmental risk assessment of trace metal pollution: A statistical perspective. *Environmental Geochemistry and Health*, 47(4), 94. [\[DOI\]](#)
- Pancholi, K.C., Singh, P.J., Bhattacharyya, K., Tiwari, M., Sahu, S.K., Vincent, T. and Kaushik, C.P., 2022. Elemental analysis of residual ash generated during plasma incineration of cellulosic, rubber and plastic waste. *Waste Management & Research*, 40(6), pp.665-675. [\[DOI\]](#)
- Panda, B.P., Kumari, R., Pradhan, A., Majhi, B.K., Acharya, P. and Parida, S.P., 2025. Assessing the bioaccumulation of copper and zinc using bird as bioindicator in different wetland ecosystems of Odisha, India. *Environmental Systems Research*, 14(1), 10. [\[DOI\]](#)
- Rahman, S.U., Qin, A., Zain, M., Mushtaq, Z., Mehmood, F., Riaz, L. and Shehzad, M., 2024. Pb uptake, accumulation and translocation in plants: Plant physiological, biochemical and molecular response: A review. *Heliyon*, 10(6), e27748.
- Rasul, A.K., Fatah, K.K., Hamed, M.H. and Tobia, F.H., 2026. Evaluation of trace metal pollution and ecological risk in the soils of Koy Sanjaq, Northeastern Iraq. *Iraqi Geological Journal*, 59(1B), pp.36-60. [\[DOI\]](#)
- Rudnick, R.L. and Gao, S., 2003. Composition of the continental crust. *Treatise on Geochemistry*, 3, pp.1-64. [\[DOI\]](#)
- Rastmanesh, F., Farrash-Alvar, S. and Shalhaf, F., 2024. Concentration of heavy metals in soil and leaves of *Conocarpus erectus* tree: A biomonitoring study, Ahvaz, Iran. *Environmental Monitoring and Assessment*, 196, 579. [\[DOI\]](#)

- Salam, M., Viantika, N.M., Amiruddin, A., Pinontoan, F.M. and Rahmatullah, R.A., 2021. The effect of bioremediation on heavy metal contaminated soil using indigenous microorganisms. *IOP Conference Series: Earth and Environmental Science*, 681(1), 012115.
- Shartooh, S.M., Najeeb, L.M. and Sirhan, M.M., 2018. Biological treatment of carcinogenic acrylonitrile using *Pseudomonas aeruginosa* in Basra city. *Journal of Biological Sciences*, 18(8), pp.415-424. [DOI]
- Skuzza, L., Szućko-Kociuba, I., Filip, E. and Božek, I., 2022. Natural molecular mechanisms of plant hyperaccumulation and hypertolerance towards heavy metals. *International Journal of Molecular Sciences*, 23(16), 9335. [DOI]
- Skvarekova, E., Tausova, M., Senova, A., Wittenberger, G. and Novakova, J., 2021. Statistical evaluation of quantities measured in the detection of soil air pollution of the environmental burden. *Applied Sciences*, 11(7), 3294. [DOI]
- Somadas, P. and Sarvade, P.G., 2025. An overview of the impacts of various industrial and urban wastes on soil properties: Contamination and remediation strategies. *Environmental Research Communications*, 7(3), 032002. [DOI]
- Szwalec, A., Mundała, P., Kędzior, R. and Pawlik, J., 2020. Monitoring and assessment of cadmium, lead, zinc and copper concentrations in arable roadside soils in terms of different traffic conditions. *Environmental Monitoring and Assessment*, 192(3), 155. [DOI]
- Tang, M., Chen, K., Rudnick, R.L. and Wang, Z., 2019. The composition of the upper continental crust: Insights from the chemical weathering of sedimentary rocks. *Geochimica et Cosmochimica Acta*, 258, pp.1-15.
- Tnoumi, A., Angelone, M., Armiento, G., Caprioli, R., Crovato, C., De Cassan, M., Montereali, M.R., Nardi, E., Parrella, L., Proposito, M., Schirone, A., Spaziani, F. and Zourarah, B., 2022. Heavy metal content and potential ecological risk assessment of sediments from Khnifiss Lagoon National Park, Morocco. *Environmental Monitoring and Assessment*, 194(6), 356. [DOI]
- Tomlinson, D.L., Wilson, J.G., Harris, C.R. and Jeffrey, D.W., 1980. Problems in the assessment of heavy-metal levels in estuaries and the formation of a pollution index. *Helgoländer Meeresuntersuchungen*, 33(1), pp.566-575. [DOI]
- Valko, M., Morris, H. and Cronin, M.T.D., 2005. Metals, toxicity and oxidative stress. *Current Medicinal Chemistry*, 12(10), pp.1161-1208. [DOI]
- Vardhan, K.H., Kumar, P.S. and Panda, R.C., 2019. A review on heavy metal pollution, toxicity and remedial measures: Current trends and future perspectives. *Journal of Molecular Liquids*, 290, 111197. [DOI]
- WHO, 1996. *Permissible Limits of Heavy Metals in Soil and Plants*. World Health Organization, Geneva, Switzerland.
- Xie, X., Liu, Y., Qiu, H. and Yang, X., 2023. Quantifying ecological and human health risks of heavy metals from different sources in farmland soils within a typical mining and smelting industrial area. *Environmental Geochemistry and Health*, 45(8), pp.5669-5683. [DOI]
- Xuefeng, L., Qiang, L., Shaolan, H., Shilai, Y., Deyu, H., Zhitao, W., Rangjin, X., Yongqiang, Z. and Lie, D., 2016. Estimation of carbon and nitrogen contents in citrus canopy by low-altitude remote sensing. *International Journal of Agricultural and Biological Engineering*, 9(5), pp.149-157. [DOI]
- Zhang, C., 2024. *Fundamentals of Environmental Sampling and Analysis*. John Wiley & Sons. ISBN: 978-1-394-24462-1.
- Zurek-Ost, M.A., Phillips, K.A., Williams, A.J., Edelman-Muñoz, A., Charest, N., Handa, S. and Isaacs, K.K., 2025. ExpoPath: A method for identifying and annotating exposure pathways from chemical co-occurrence networks. *Science of the Total Environment*, 979, 179465. [DOI]

